Chapter 4

Dynamical Simulations

This chapter presents all simulations that are required for modeling the solar system formation in Chapter 3. The simulations are generated by the mathematical program Maple 9. This program has more powerful tools to simulate a small dynamical system which already known equation of motion. Almost all simulations in this chapter are the constructing system of nonlinear second-order differential equations, which must be solved by numerical method. For this work, the Runge-Kutta method, provided by Maple, is applied with more accuracy and precision. The aspect of Maple 9 classic worksheet is shown in Figure 4.1 below.

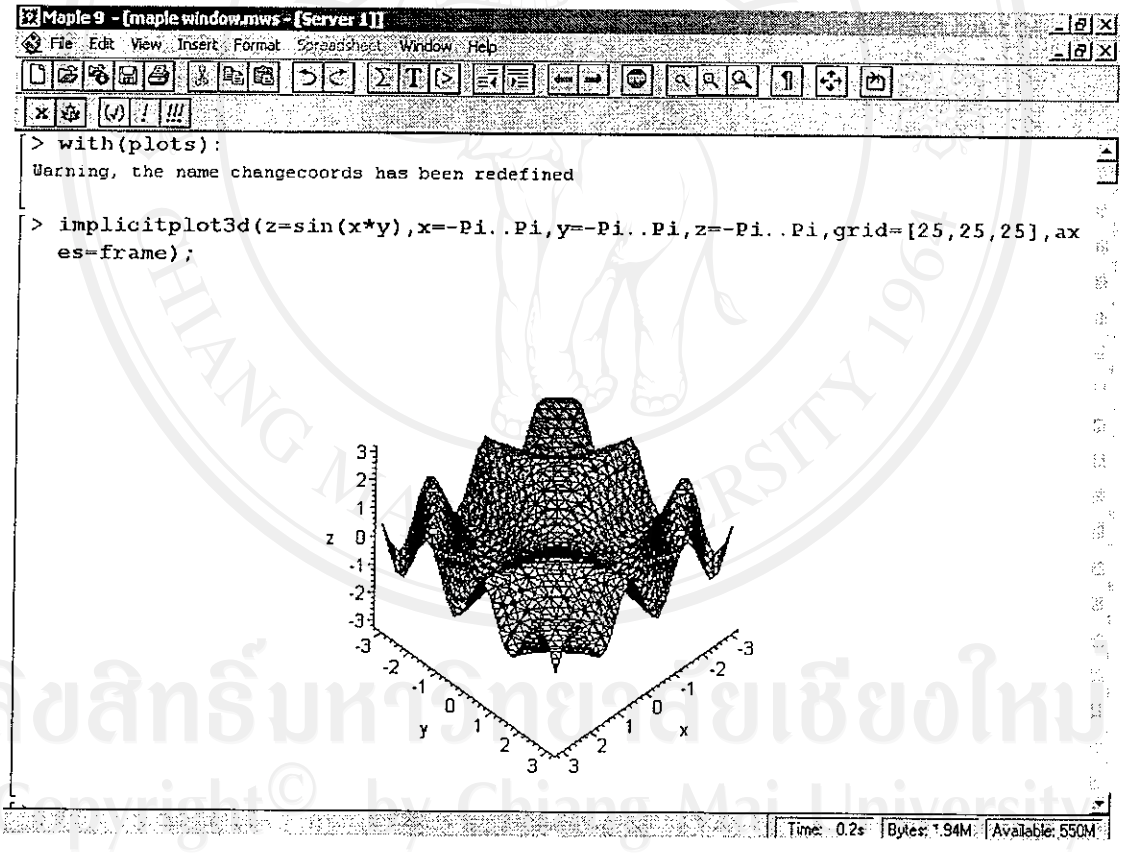

Figure 4.1 Maple 9 classic worksheet with "implicitplot3d" command.

The units that are used in all simulation are the unit of the Earth: the length is in *Astronomical Unit (AU)*, the time is in *year (yr)*, and the mass is in *Earth Unit (EU)*. Then the gravitational constant is

$$
\begin{aligned}
\mathrm{G} &= 6.67\times10^{-11}\, N\cdot m^2/kg^2 \\
&= 6.67\times10^{-11}\, m^2/kg\cdot s^2 \\
&= 6.67\times10^{-11}\,\frac{\left(\dfrac{AU}{1.495979\times10^{11}}\right)^3}{\left(\dfrac{EU}{5.976\times10^{24}}\right)\cdot\left(\dfrac{yr}{365\times24\times60\times60}\right)^2} \\
&= 1.184\times10^{-4}\, AU^3/EU\cdot yr^2
\end{aligned}
\tag{4.1}
$$

These units are more useful than SI units in that the number involved is much less.

4.1 The Orbital Elastic Collision

4.1.1 New Orbit of Particles

After collision, each particle will have a new orbit, which carries new angular momentum and total energy. From Section 2.2, we can determine a new orbit of particle by using the Equation 2.16 to find α and ε, then substitute into

$$r = \frac{\alpha}{1-\varepsilon\cos(\theta-\phi)} \tag{4.2}$$

where ϕ is the phase angle of orbit relative to the x axis.

Firstly, we must know the collision points that two orbit are intersected by solving equation

$$r_1(\theta) - r_2(\theta) = 0 \tag{4.3}$$

for θ. This equation can be solved easily by the command "`solve();`" in Maple. The solution must be two real values or two imaginary values if the orbits are not intersected. We can check these solutions by plotting as shown in Appendix (New Orbits of Particles). Note that, the solve command can be executed only when one of phase angle is set to be zero. All processes of evaluating the new orbits are presented as a chart in Figure 4.2.

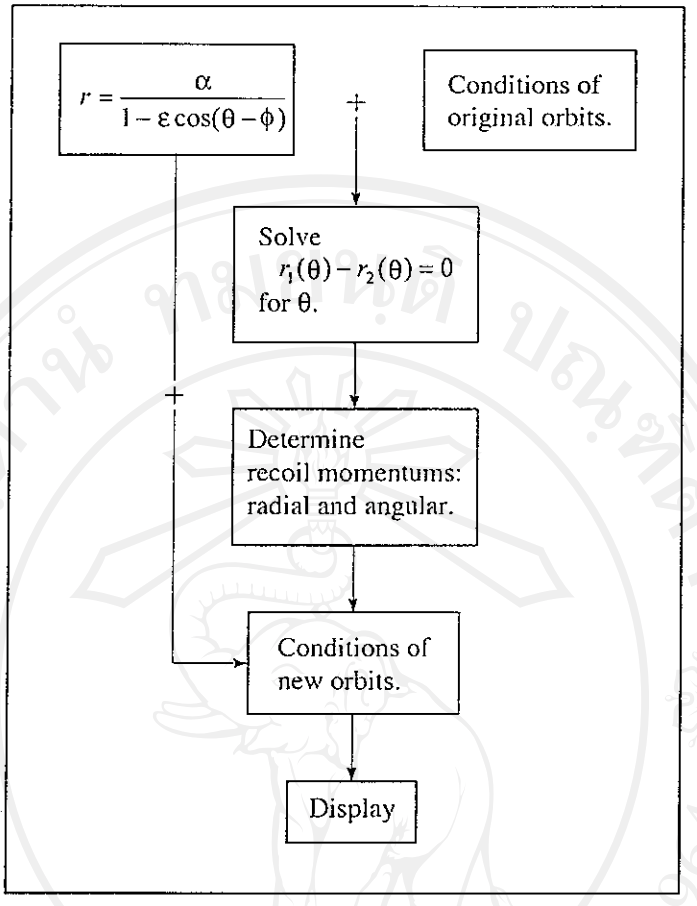

Figure 4.2 The processes of evaluating the new orbit of particles.

The simulation results of orbital collision between

$$\text{particle}\,1 \rightarrow m_1 = 0.5,\ \ell_1^{ori} = 1.0,\ \varepsilon_1 = 0.40 \qquad (4.4a)$$

and

$$\text{particle}\,2 \rightarrow m_2 = 1.0,\ \ell_2^{ori} = 1.0,\ \varepsilon_2 = 0.85 \qquad (4.4b)$$

moving around central mass $M = G^{-1} = 8445.95\,EU$ with various phase difference $\Delta\phi$ are shown in Figure 4.3.

All simulation results show us that the new orbits depend on phase difference or, in the other hand, the orientation of original orbits. The angular momentum of recoil particles, however, is independent with orbital orientation: from this simulation $\ell^{ori} = 1.0$ and $\ell^{rec} = 0.2$ for all cases. Therefore, it is a good quantity for indicating how close the particle does from the center.

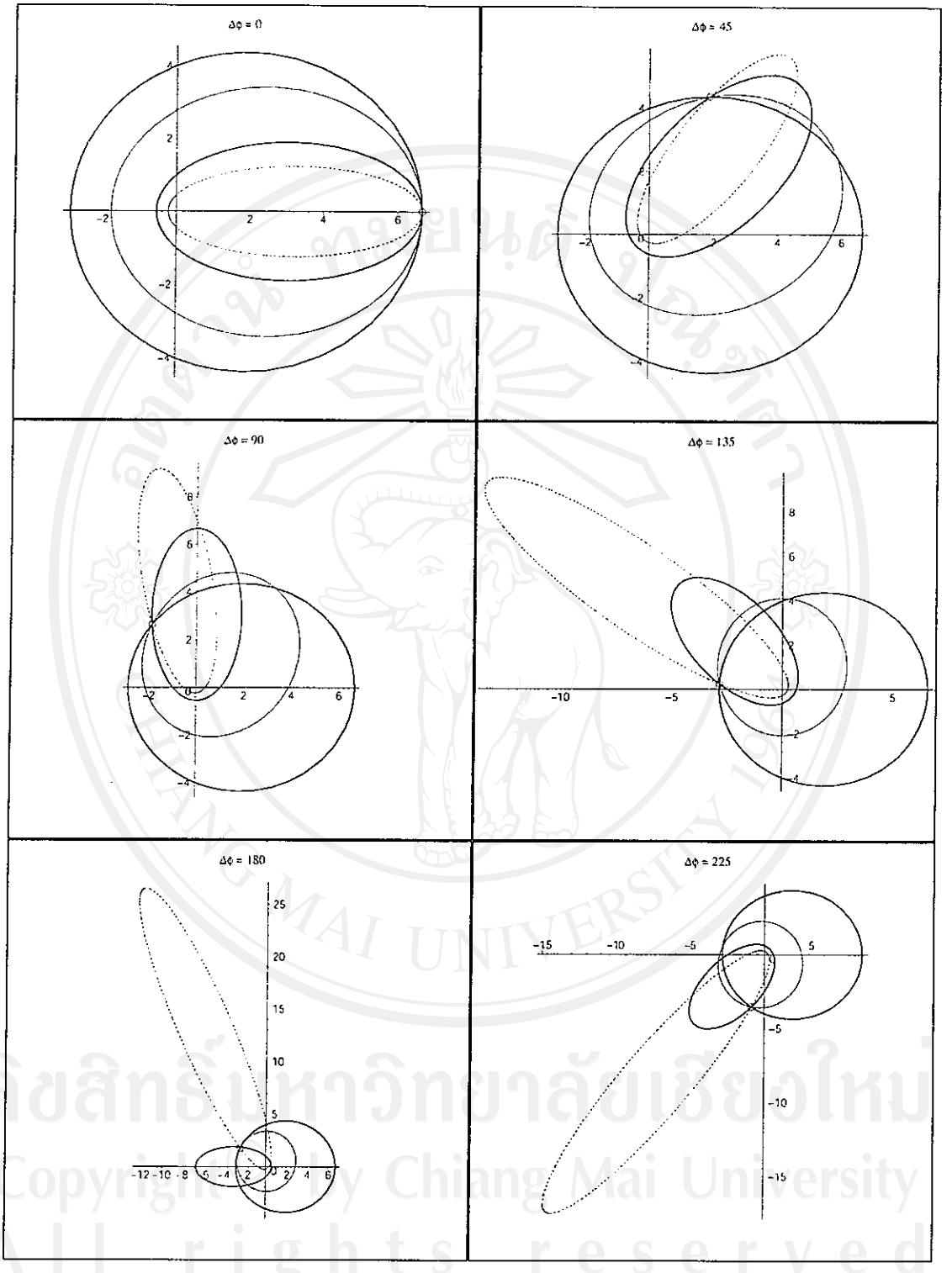

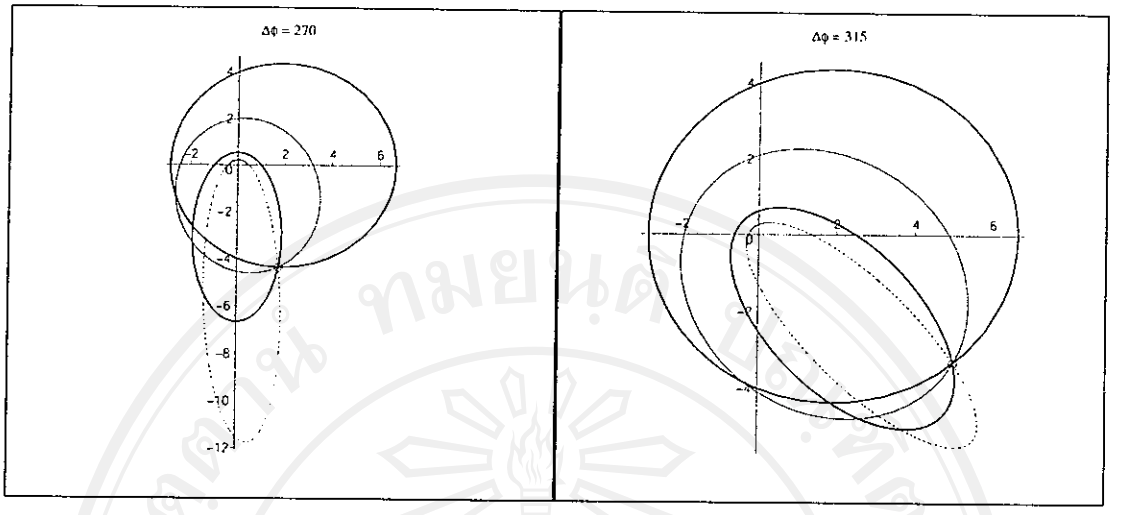

Figure 4.3 Simulation results of orbital collision between two particles. The original orbits are presented by thick line; the fixed-bigger ellipse is of particle 1. The thin dash line and the thin solid line are the new orbit of particle 1 and particle 2 respectively. The collision point is enclosed by a small circle.

4.1.2 Two-Real-Body Approach

The orbital elastic collision between two spherical bodies, radius a and mass m_1 and m_2, can be simulated by adding the force of rigidity to the equation of motion. This force is repulsive that switch from 0 to ∞ at the surface of the object (Figure 4.4); it presents the rigidity or the incompressibility of real object.

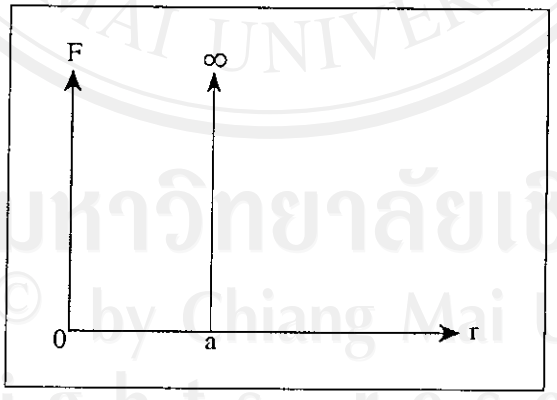

Figure 4.4 Graph of the force of rigidity.

It will be more convenient if we fix the massive central mass at the origin. The Keplerion motion of both objects around the center can be considered as the motion of test mass. The equation of motion of both objects can be written as

$$\frac{d^2\mathbf{r}_1}{dt^2} = -\frac{GM}{r_1^3}\mathbf{r}_1 + f(\mathbf{r}_{12})\frac{Gm_2}{a^3}\mathbf{r}_{12} \tag{4.5a}$$

and

$$\frac{d^2\mathbf{r}_2}{dt^2} = -\frac{GM}{r_2^3}\mathbf{r}_2 + f(\mathbf{r}_{12})\frac{Gm_1}{a^3}\mathbf{r}_{21} \tag{4.5b}$$

where

$$f(\mathbf{r}) = \begin{cases} 0 & ,|\mathbf{r}| > a \\ \infty & ,|\mathbf{r}| \le a \end{cases} \tag{4.6}$$

is the rigidity factor or switching function.

In computation, the program can not compute at ∞, so it is sufficient to use some large number, $\sim 10^6 - 10^8$; note that, this value must be considered as proportional to the radius a of particle. The switching function $f(\mathbf{r})$ can be assigned in Maple as

```
>f:=r->piecewise(r<=a,1e6,1);
```

The codes can be executed faster if we use the rectangular coordinate or in term of x and y. Thus, the equation 4.5a and 4.5b can be written as

$$\frac{d^2x_1}{dt^2} = -\frac{GMx_1}{(x_1^2+y_1^2)^{\frac{3}{2}}} + \frac{Gm_2(x_1-x_2)}{a^3} f\left(\sqrt{(x_1-x_2)^2+(y_1-y_2)^2}\right) \tag{4.7a}$$

$$\frac{d^2y_1}{dt^2} = -\frac{GMy_1}{(x_1^2+y_1^2)^{\frac{3}{2}}} + \frac{Gm_2(y_1-y_2)}{a^3} f\left(\sqrt{(x_1-x_2)^2+(y_1-y_2)^2}\right) \tag{4.7b}$$

and

$$\frac{d^2x_2}{dt^2} = -\frac{GMx_2}{(x_2^2+y_2^2)^{\frac{3}{2}}} + \frac{Gm_2(x_2-x_1)}{a^3} f\left(\sqrt{(x_1-x_2)^2+(y_1-y_2)^2}\right) \tag{4.8a}$$

$$\frac{d^2y_2}{dt^2} = -\frac{GMy_2}{(x_2^2+y_2^2)^{\frac{3}{2}}} + \frac{Gm_2(y_2-y_1)}{a^3} f\left(\sqrt{(x_1-x_2)^2+(y_1-y_2)^2}\right) \tag{4.8b}$$

Finding the initial conditions, which can bring both particles collide at collision point, has a bit of difficulty. However, it can be shown as a processing diagram in Figure 4.5.

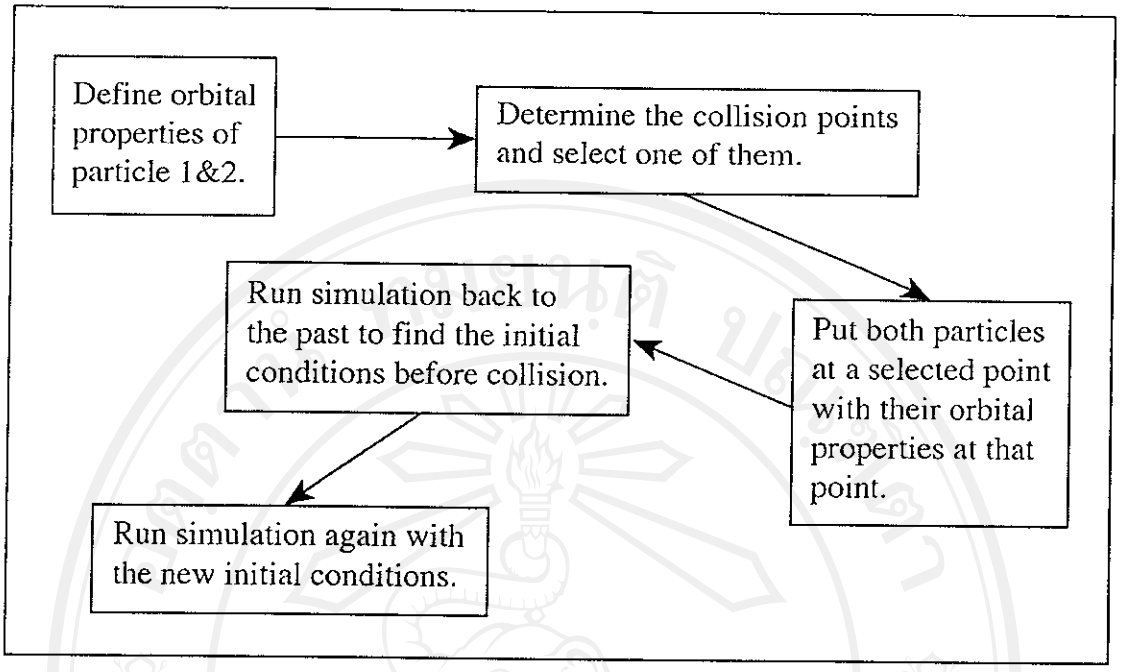

Figure 4.5 Processing diagram of finding initial conditions before collision.

Collision between two real objects radius $a = 0.05$, phase different $\Delta\phi = 45$, and the rest of initial conditions are the same as the particles in Section 4.1.1, can be simulated with the results illustrated in Figure 4.6.

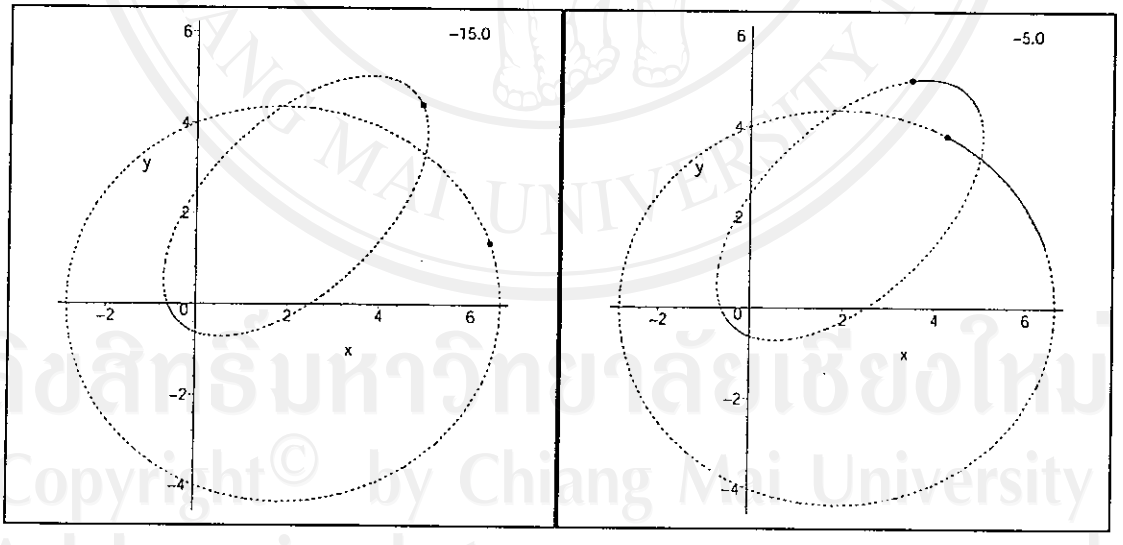

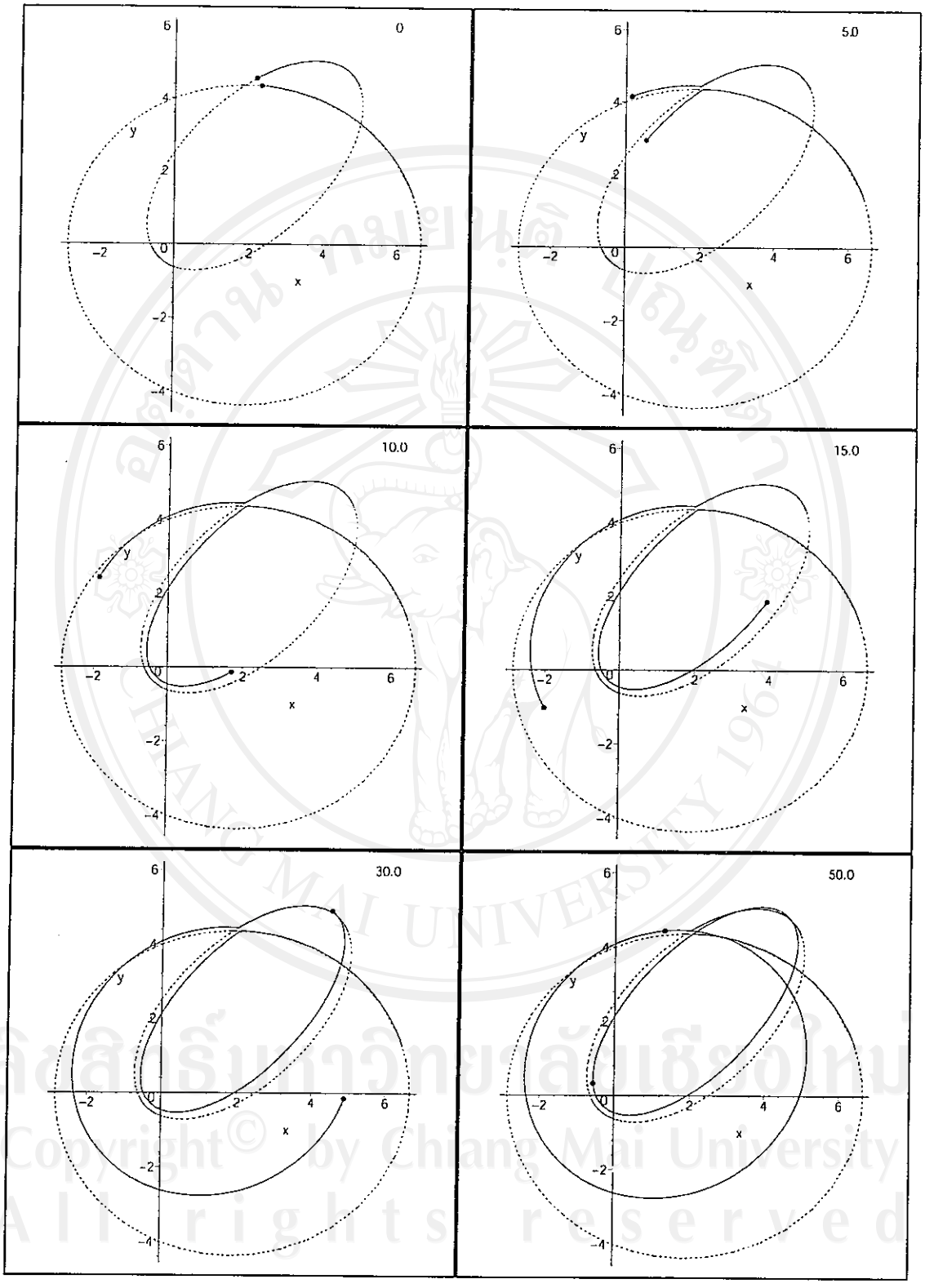

Figure 4.6 Simulation result of two-real-body collision radius $a = 0.05$, phase different $\Delta\phi = 45$, and with the same initial conditions as the particles in Section 4.1.1. Original orbits are shown in dash line.

The result of this simulation is look like the result in Figure 4.3, in the case of $\Delta\phi = 45$. However, the angular momentum is not totally transferred; this may be the effect of dimension of the objects.

4.2 The Orbital Motion in the Resisting Medium

4.2.1 Coplanar Motion

From Section 2.3, equation of motion of the object moving in a rotating disk cloud can be written as

$$\frac{d^2\mathbf{r}}{dt^2} = -\frac{GM}{r^3}\mathbf{r} - \frac{1}{2}\frac{c\rho A}{m}|\mathbf{v}-\mathbf{u}|^2\frac{(\mathbf{v}-\mathbf{u})}{|\mathbf{v}-\mathbf{u}|} \tag{4.9}$$

or

$$\frac{d^2\mathbf{r}}{dt^2} = -\frac{GM}{r^3}\mathbf{r} - \frac{1}{2}\frac{c\rho A}{m}|\mathbf{v}-\mathbf{u}|(\mathbf{v}-\mathbf{u}) \tag{4.10}$$

Here we use the Prandtl expression to express the retarding force.

We cannot simulate this interaction, however, by the real conditions, even we can estimate, because it may take long time to run on personal computer. Thus, the suitable conditions are decided to use for appreciating this interaction with careless about the real system.

It will be more convenient if we define a new coefficient κ by

$$\kappa = \frac{1}{2}\frac{c\rho A}{m} \tag{4.11}$$

and the velocity field $\mathbf{u}$ by

$$\begin{aligned}\mathbf{u} &= \sqrt{\frac{GM}{r}}\left(-\sin\theta\,\hat{x} + \cos\theta\,\hat{y}\right)\\ &= \sqrt{\frac{GM}{\sqrt{x^2+y^2}}}\left(-\frac{y}{\sqrt{x^2+y^2}}\hat{x} + \frac{x}{\sqrt{x^2+y^2}}\hat{y}\right)\\ &= -\frac{\sqrt{GM}\,y}{(x^2+y^2)^{\frac{3}{4}}}\hat{x} + \frac{\sqrt{GM}\,x}{(x^2+y^2)^{\frac{3}{4}}}\hat{y}\end{aligned} \tag{4.12}$$

The aspect of rotating disk cloud with this velocity field is shown in Figure 4.7.

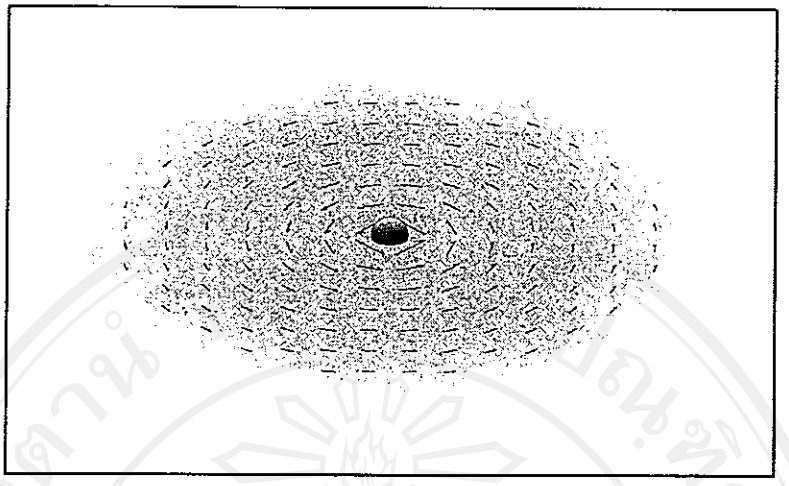

Figure 4.7 Rotating disk cloud and velocity field.

Then, Equation 4.10 can be written as

$$\frac{d^2x}{dt^2} = -\frac{GMx}{(x^2+y^2)^{\frac{3}{2}}} - \kappa\left|\frac{dx}{dt} + \frac{\sqrt{GM}\,y}{(x^2+y^2)^{\frac{3}{4}}}\right|\left(\frac{dx}{dt} + \frac{\sqrt{GM}\,y}{(x^2+y^2)^{\frac{3}{4}}}\right) \qquad (4.13a)$$

and

$$\frac{d^2y}{dt^2} = -\frac{GMy}{(x^2+y^2)^{\frac{3}{2}}} - \kappa\left|\frac{dy}{dt} - \frac{\sqrt{GM}\,x}{(x^2+y^2)^{\frac{3}{4}}}\right|\left(\frac{dy}{dt} - \frac{\sqrt{GM}\,x}{(x^2+y^2)^{\frac{3}{4}}}\right) \qquad (4.13b)$$

Simulation result of the system, which central mass $M = G^{-1}EU$, $\kappa = 0.2$ and launching object at $x = 2, y = 0$ with initial velocities $v_x = 0, v_y = 0.5$, is illustrated in Figure 4.8.

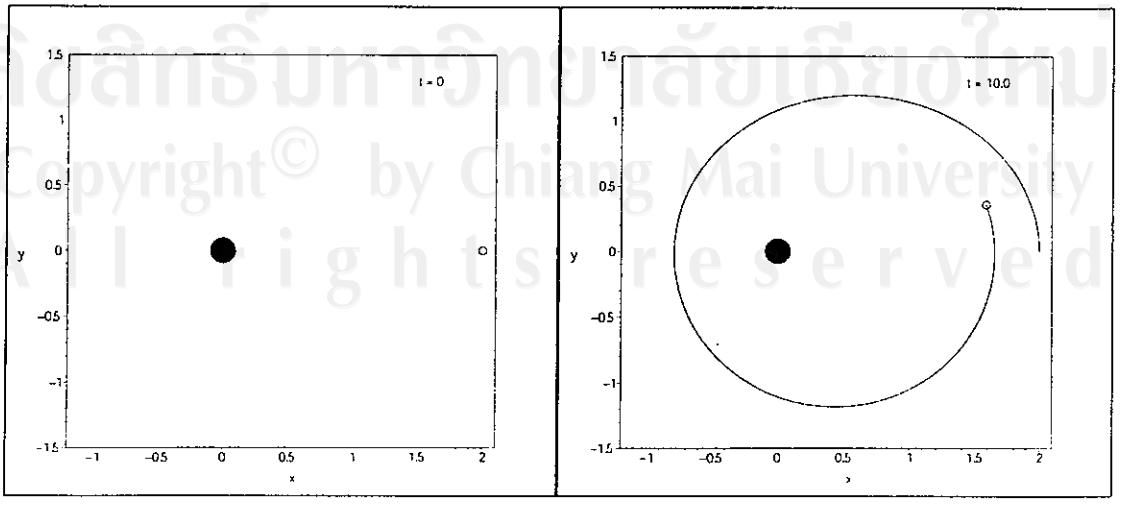

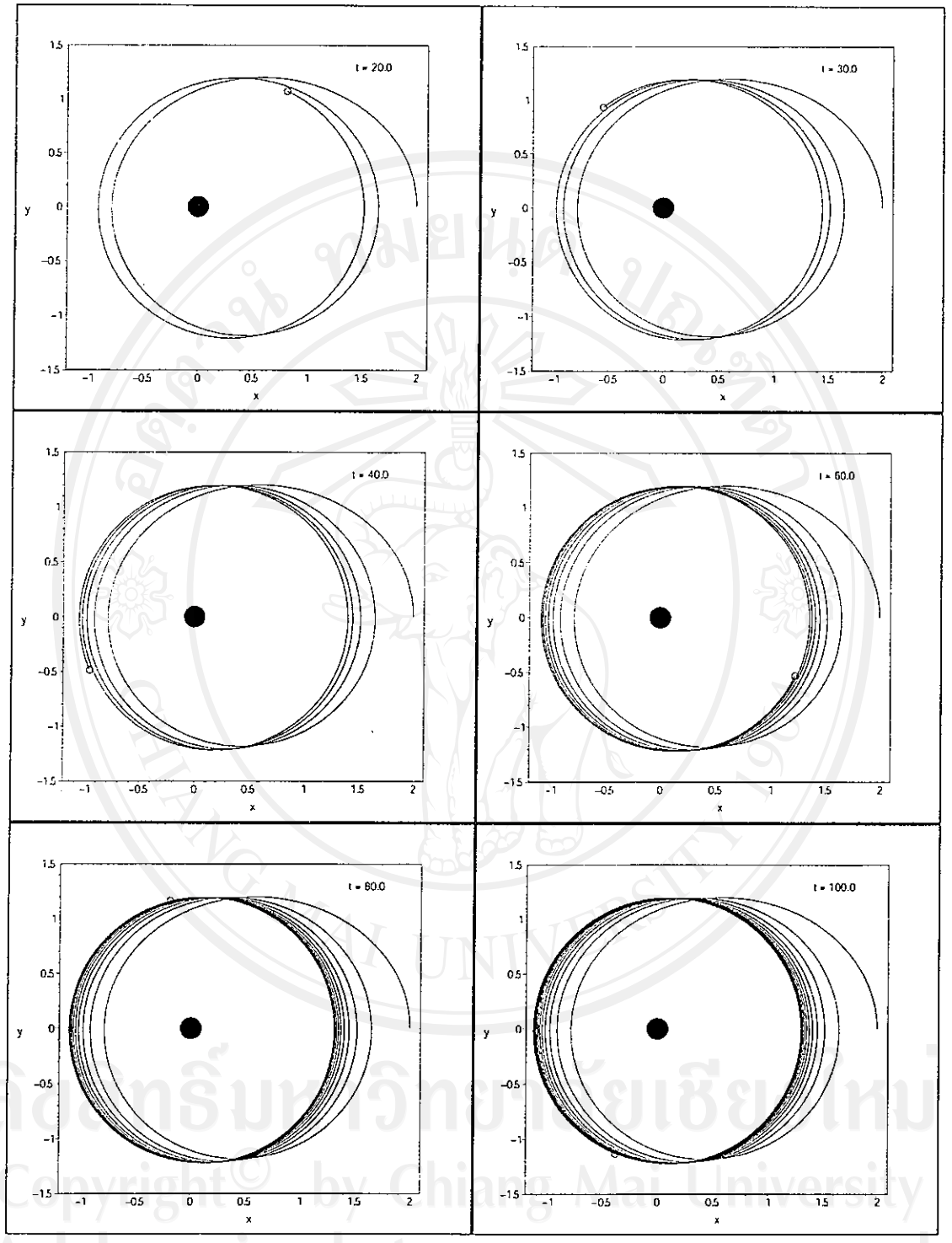

Figure 4.8 Simulation result of motion in resisting medium, $\kappa = 0.2$, from $t = 0$ to $t = 100yr$.

From this simulation, we see that the orbit of the object is decreased and adjusted to be more circular belong to the velocity field direction. As mentioned in Section 3.3.2, the orbit of planet may be adjusted by this process.

4.2.2 Non-Coplanar Motion

The object, which moving through a plane of resisting medium, will be mainly retarded in vertical component, because there is no velocity field in this component. Thus, the effect of retarding force is proportional to the thickness of the disk. The simulation must be considered in three dimensions then the equation of motion can be written as

$$\frac{d^2x}{dt^2} = -\frac{GMx}{(x^2+y^2+z^2)^{\frac{3}{2}}} - \kappa\left|\frac{dx}{dt} + \frac{\sqrt{GM}\,y}{(x^2+y^2)^{\frac{3}{4}}}\right|\left(\frac{dx}{dt} + \frac{\sqrt{GM}\,y}{(x^2+y^2)^{\frac{3}{4}}}\right)Disk(z) \quad (4.14a)$$

$$\frac{d^2y}{dt^2} = -\frac{GMy}{(x^2+y^2+z^2)^{\frac{3}{2}}} - \kappa\left|\frac{dy}{dt} - \frac{\sqrt{GM}\,x}{(x^2+y^2)^{\frac{3}{4}}}\right|\left(\frac{dy}{dt} - \frac{\sqrt{GM}\,x}{(x^2+y^2)^{\frac{3}{4}}}\right)Disk(z) \quad (4.14b)$$

and

$$\frac{d^2z}{dt^2} = -\frac{GMz}{(x^2+y^2+z^2)^{\frac{3}{2}}} - \kappa\left|\frac{dz}{dt}\right|\left(\frac{dz}{dt}\right)Disk(z) \quad (4.14c)$$

where

$$Disk(z) = \begin{cases} 0 & ,|z| > \dfrac{thickness}{2} \\ 1 & ,|z| \le \dfrac{thickness}{2} \end{cases} \quad (4.15)$$

The purpose of defining function $Disk(z)$ is to specify the boundary of the rotating disk; for example, the retarding force vanishes when $|z| > thickness/2$.

Simulation result of the system, which central mass $M = G^{-1}EU$, $\kappa = 0.2$, thickness $0.2AU$, and with the object launched at $x = \sqrt{3}, y = 0, z = 1$ (or inclined 30 degree) with initial velocities $v_x = 0, v_y = 0.5, v_z = 0$, is illustrated in Figure 4.8.

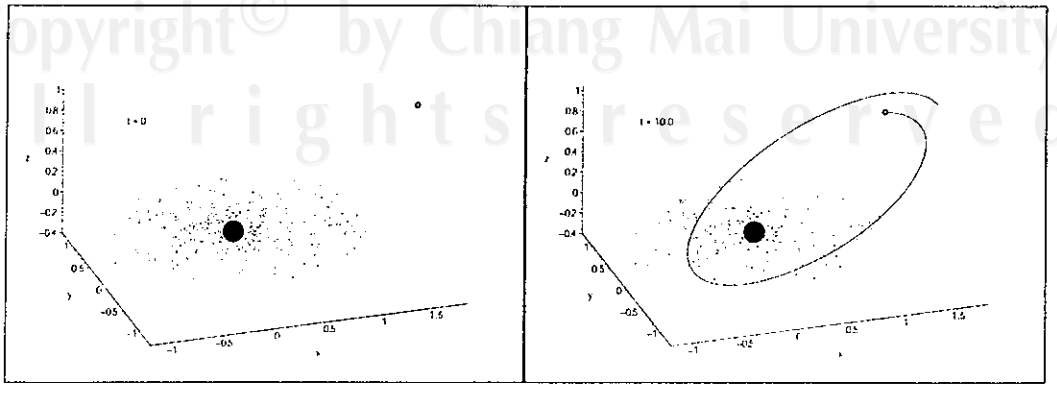

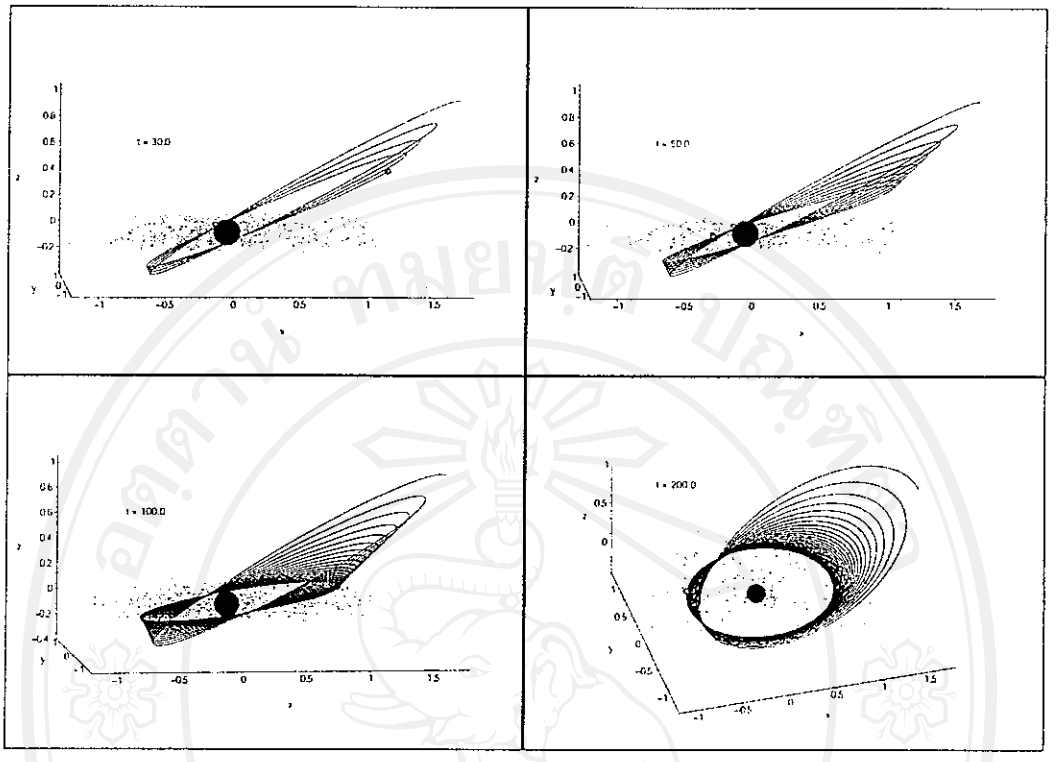

Figure 4.9 Simulation result of non-coplanar object moving through a disk of resisting medium, $\kappa = 0.2$, thickness $0.2AU$, from $t = 0$ to $t = 200yr$.

This result shows us that the role of resisting medium can also bring non-coplanar motion into a plane together with more circular. Therefore, the coplanar motion of planets may be induced by this process, as mentioned in Section 3.3.2.

4.3 The Tidal Induction

Simulation of tidal induction between two clusters of particles can be constructed by reducing many-body system to be a system of three-body. The reason is to decrease the time used in simulation and, furthermore, gravitational interaction between particles can be neglected when the tidal induction begin. The aspect of the system is shown in Figure 4.10.

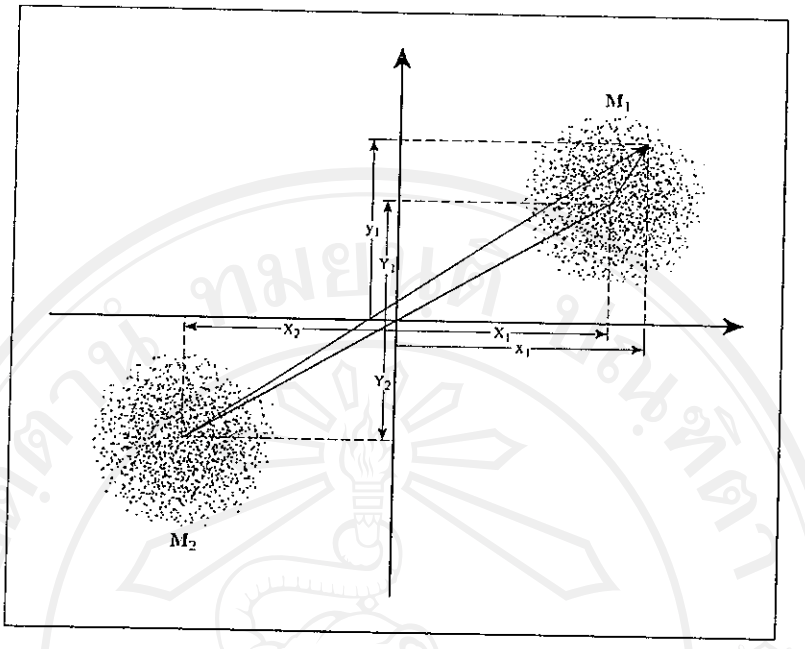

Figure 4.10 Two clusters before interacting each other with tidal force.

The equations of motion of cluster M_1, M_2 and the test mass can be written as

$$\frac{d^2X_1}{dt^2} = -\frac{GM_2(X_1 - X_2)}{\left((X_1 - X_2)^2 + (Y_1 - Y_2)^2\right)^{\frac{3}{2}}} \tag{4.16a}$$

$$\frac{d^2Y_1}{dt^2} = -\frac{GM_2(Y_1 - Y_2)}{\left((X_1 - X_2)^2 + (Y_1 - Y_2)^2\right)^{\frac{3}{2}}} \tag{4.16b}$$

$$\frac{d^2X_2}{dt^2} = -\frac{GM_1(X_2 - X_1)}{\left((X_1 - X_2)^2 + (Y_1 - Y_2)^2\right)^{\frac{3}{2}}} \tag{4.17a}$$

$$\frac{d^2Y_2}{dt^2} = -\frac{GM_1(Y_2 - Y_1)}{\left((X_1 - X_2)^2 + (Y_1 - Y_2)^2\right)^{\frac{3}{2}}} \tag{4.17b}$$

and

$$\frac{d^2x}{dt^2} = -\frac{GM_1(x - X_1)}{\left((x - X_1)^2 + (y - Y_1)^2\right)^{\frac{3}{2}}} - \frac{GM_2(x - X_2)}{\left((x - X_2)^2 + (y - Y_2)^2\right)^{\frac{3}{2}}} \tag{4.18a}$$

$$\frac{d^2y}{dt^2} = -\frac{GM_1(y - Y_1)}{\left((x - X_1)^2 + (y - Y_1)^2\right)^{\frac{3}{2}}} - \frac{GM_2(y - Y_2)}{\left((x - X_2)^2 + (y - Y_2)^2\right)^{\frac{3}{2}}} \tag{4.18b}$$

In this simulation, the mass of both cluster are set to be equal, $M_1 = M_2 = M$; the Lagrange point L_1 is therefore at origin. The initial condition of test masses are given by the ring construction conditions that construct the test masses as a ring around mass M_1 and M_2 with initial velocity given by the circular velocity:

$$\upsilon_{cir} = \sqrt{\frac{GM}{r_{ring}}} \tag{4.16}$$

After both clusters have launched, the interactions begin as they approach the pericenter. The tidal induction is dominated, whether high-density-regions induction or mass transfer can occur. The simulation of high-density-regions induction can be constructed by using two clusters mass $M = 0.1G^{-1}\,EU$, radius $a = 0.44, 0.45$ and $0.46AU$ (three rings), launched at $X_1 = 5, Y_1 = 0$ and $X_2 = -5, Y_2 = 0$ with velocities $u_1 = 0, v_1 = 0.035$ and $u_2 = 0, v_2 = -0.035$. These conditions give us two elliptical orbits, which equal eccentricity $\varepsilon_1 = \varepsilon_2 = 0.75$ and pericenter $r_{min1} = r_{min2} = 0.714 > a$. Simulation results are shown in Figure 4.11.

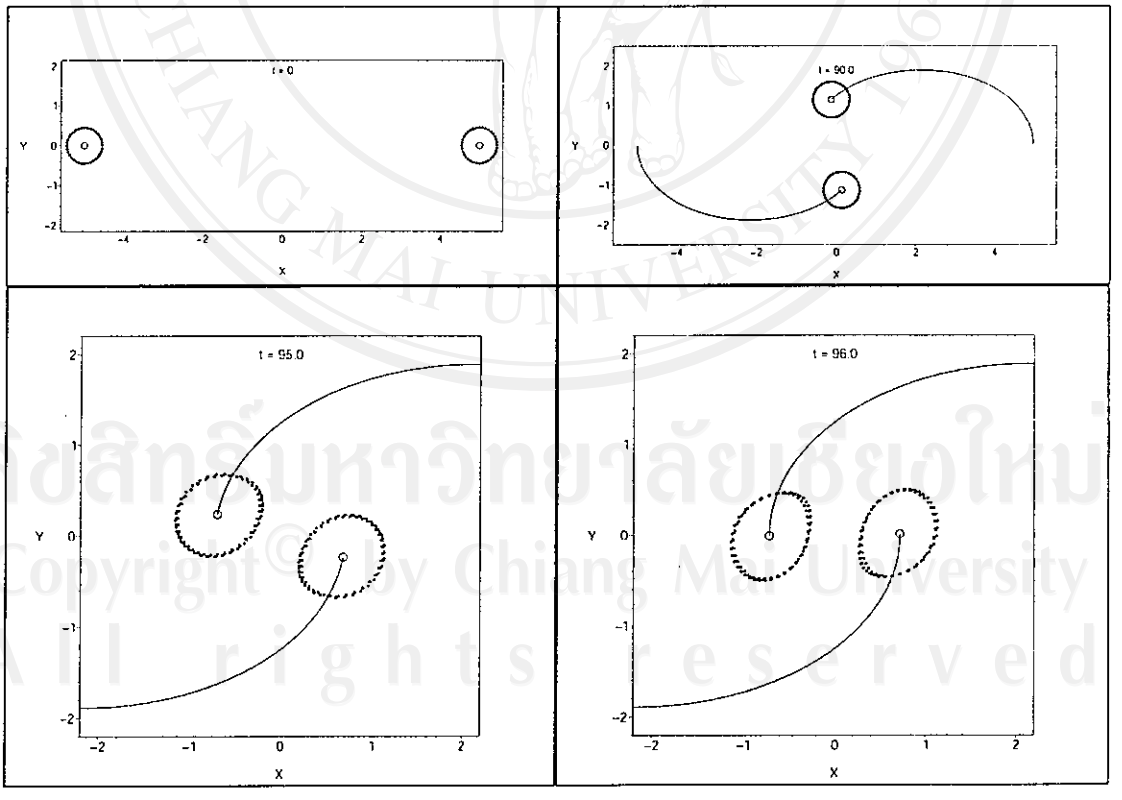

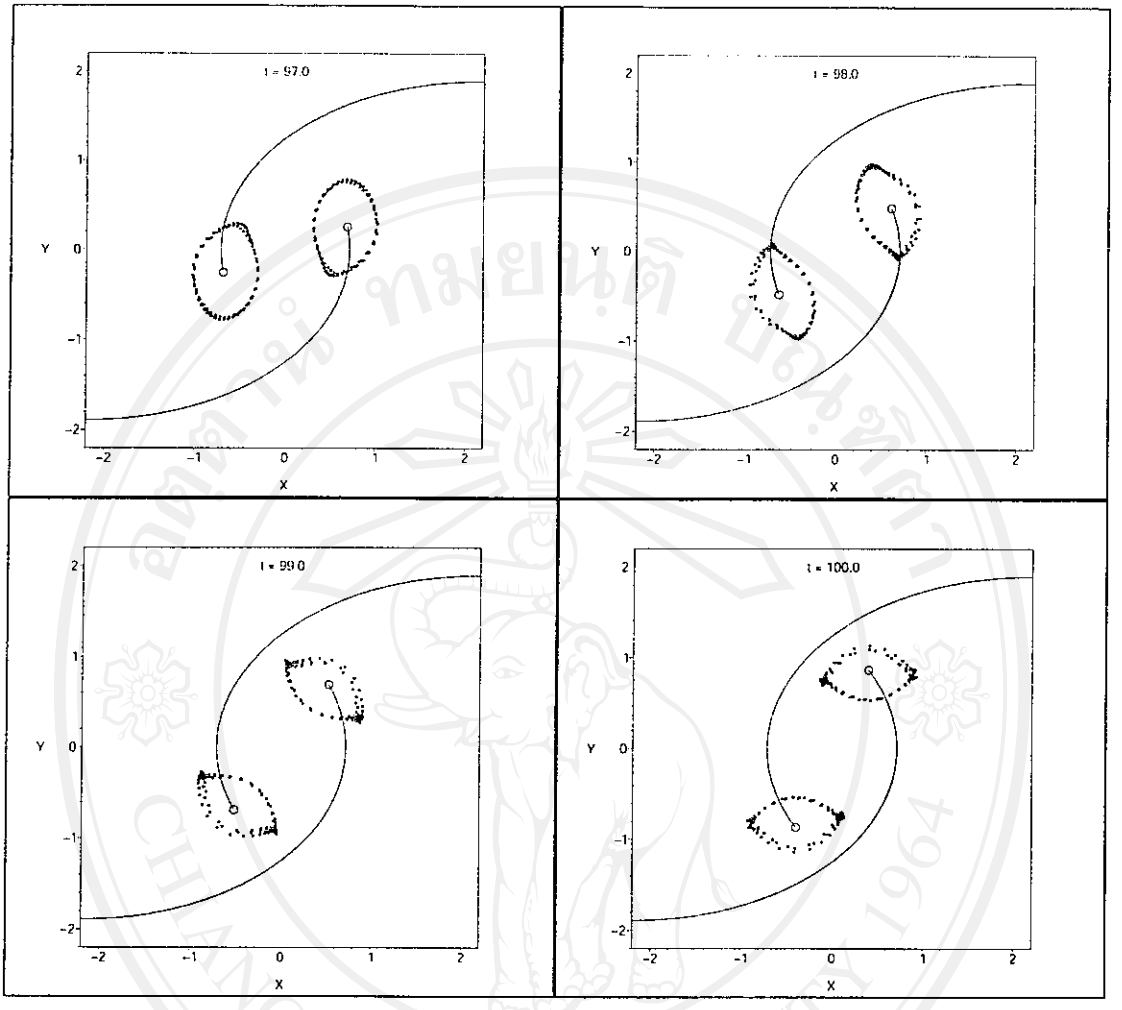

Figure 4.11 Simulation result of high-density-regions induction of two equal mass clusters; the rings construction of particles are collapsed into two regions.

In the case that both clusters are different in mass and size, the tidal induction may stronger when they close together. This case is similar to when the protoplanet reached its pericenter near protosun; the protoplanet may be induced to collapse strongly into two regions. The simulation can be constructed by using the cluster mass $M_1 = 0.01G^{-1}\,EU$, radius $a = 0.098$, 0.100 and $0.102AU$ (three rings), launches at $X_1 = 10, Y_1 = 0$ and moves elliptically with $\varepsilon_1 = 0.61$ around mass $M_2 = G^{-1}\,EU$, which is fixed at the origin. The close-up view simulation of cluster M_1 is shown in Figure 4.12.

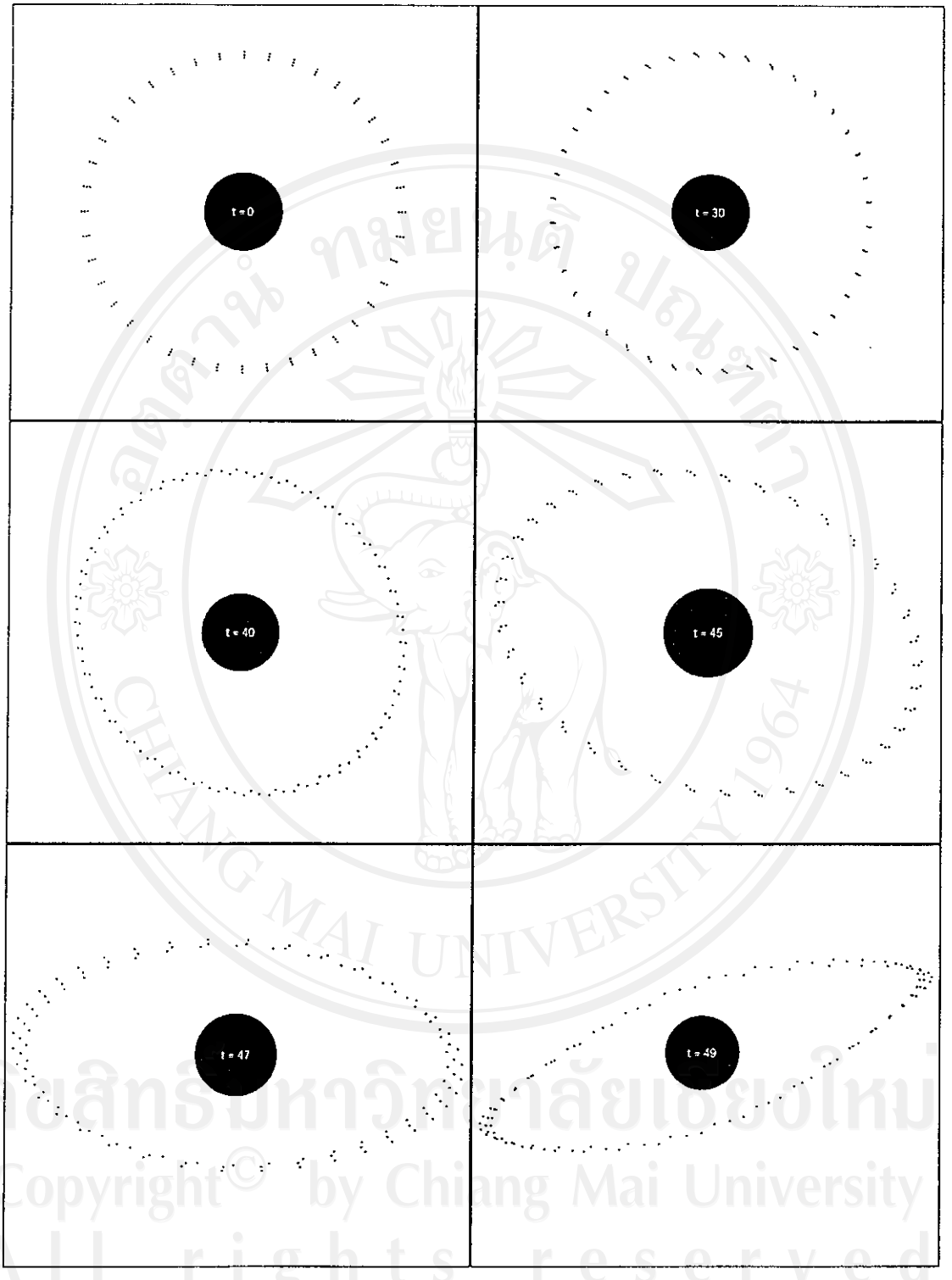

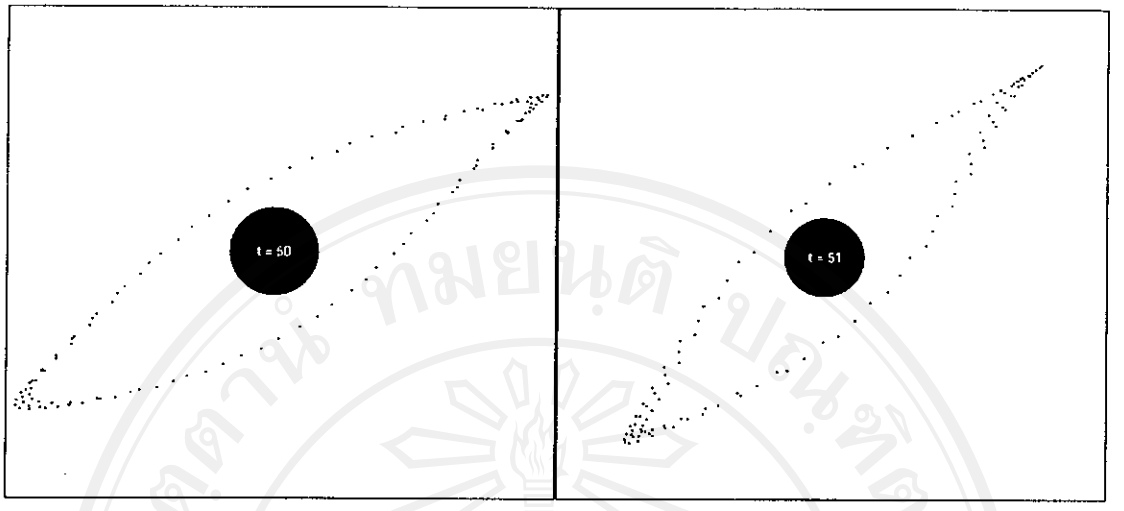

Figure 4.12 The close-up view simulation of cluster M_1, the particle rings are strongly collapsed into two regions.

In the real system, the collision of particles in both interactions must be produced heat, which can melt them together; the mass will be clumped as a molten chunks. These molten chunks may form protosatellites around protoplanet.